Signal sequence within FcγRIIA controls calcium wave propagation patterns: Apparent role in phagolysosome fusion

Randall G. Worth*, Moo-Kyung Kim*, Andrei L. Kindzelskii†, Howard R. Petty†‡§, and Alan D. Schreiber*

*Department of Medicine, University of Pennsylvania School of Medicine, Philadelphia, PA 19104; Departments of †Ophthalmology and Visual Sciences and ‡Microbiology and Immunology, University of Michigan School of Medicine, Ann Arbor, MI 48105

Edited by Seymour J. Klebanoff, University of Washington School of Medicine, Seattle, WA, and approved February 21, 2003 (received for review November 1, 2002)

Calcium oscillations and traveling calcium waves have been observed in living cells, although amino acid sequences regulating wave directionality and downstream cell functions have not been reported. In this study we identify an amino acid sequence within the cytoplasmic domain of the leukocyte IgG receptor FcγRIIA that affects the amplitude of calcium spikes and the spatiotemporal dynamics of calcium waves in the vicinity of phagosomes. By using high-speed microscopy to map calcium-signaling routes within cells, we have discovered that bound IgG-coated targets trigger two calcium waves traveling in opposite directions about the perimeter of cells expressing FcγRIIA. After phagocytosis, one calcium wave propagates around the plasma membrane to the site of phagocytosis where it splits into two calcium signals: one traveling to and encircling the phagosome once, and the second continuing around the plasma membrane to the point of origin. However, in a genetically engineered form of FcγRIIA containing a mutation in the cytoplasmic L-T-L motif, the calcium signal travels around the plasma membrane, but is not properly routed to the phagosome. Furthermore, these calcium pattern-deficient mutants were unable to support phagolysosome fusion, although recruitment of phagolysosome-associated proteins lysosome-associated protein 1, Rab5, and Rab7 were normal. Our findings suggest that: (*i*) calcium signaling is a late step in phagolysosome fusion, (*ii*) a line of communication exists between the plasma membrane and phagosome, and (*iii*) the L-T-L motif is a signal sequence for calcium signal routing to the phagosome.

Phagocytosis and phagolysosome fusion by leukocytes are crucial components of the immune response to invading pathogens (1). The recognition and destruction of IgG-coated pathogens are mediated by receptors for the Fc domain of IgG (FcγR). On binding an IgG-coated target to leukocyte FcγRs, signals are generated that orchestrate phagocytosis of a target. A key element in FcγRIIA's phagocytosis-signaling pathway is an immunoreceptor tyrosine-based activation motif (ITAM), which consists of two tyrosine-based YxxL sequences separated by a stretch of 12 aa within its intracellular region (2). Phosphorylation of ITAM tyrosine residues leads to recruitment of Src tyrosine kinases (3, 4). These phosphotyrosines constitute a Src homology 2-binding site for Syk kinases. Subsequent phosphorylation of Syk kinase leads to the recruitment and activation of various downstream effector molecules associated with phagosome maturation (5–10). Once internalized, phagosomes fuse with lysosomes containing the enzymes necessary for target degradation (1, 11–13). Phagolysosome formation is believed to require proteins such as Rab5, EEA1, rabaptin, Rab7, and lysosome-associated protein 1 (LAMP-1), as well as intracellular calcium signaling (14, 15). Although mutation of FcγRIIA's ITAM tyrosine residues abolishes its phagocytic activity, it does not affect phagolysosome formation (16). Thus, some other sequence within FcγRIIA may be responsible for phagolysosome fusion. The present study identifies a sequence of three amino acids, L-T-L, beginning at residue 315 of the cytoplasmic domain of FcγRIIA that controls calcium wave propagation patterns and phagolysosome formation within cells.

Methods

Cell Culture. Chinese hamster ovary (CHO) cells were grown in Ham's F-12 (BioWhittaker) supplemented with 10% FBS (Summit Biotechnology, Fort Collins, CO). CHO cells were transfected by FuGene-6 transfection reagent (Roche Diagnostics) with 1 μg of pcDNA3.1 containing the WT FcγRIIA or mutant FcγRIIA constructs. Permanent cell lines were selected by using 500 μg/ml G-418 (Mediatech, Herndon, VA) followed by sorting on a FACSVantage (Becton Dickinson) cell sorter. After generation of single-cell clones, colonies were picked and examined for expression. Clones of CHO cells expressing WT and mutant FcγRIIAs were selected for equivalent expression and maintained in media containing 100 μg/ml G-418.

Lysosome Labeling. Transfectants were grown on glass coverslips (Corning) overnight at 37°C. A total of 5 μg of rhodamine-conjugated dextran (10,000 molecular weight; Molecular Probes) was added to each coverslip for 90 min at 37°C. Cells were washed with PBS followed by addition of fresh media. Imaging of lysosomes was performed by using an Axiovert 35 fluorescence microscope (Zeiss) with mercury illumination. Optical filters for rhodamine excitation and emission were 530DF22 and 590DF30, respectively (Omega Optical, Brattlesboro, VT). Images were collected by using a charge-coupled device camera (Hamamatsu Photonics, Hamamatsu City, Japan).

Phagocytosis of Erythrocytes. Sheep red blood cells (Alsever; Rockland, Gilbertsville, PA) were opsonized with the highest subagglutinating concentration of IgG rabbit anti-sheep antibody (ICN). Subsequently, antibody-coated cells (EA) were added to transfectants at a target-to-effector ratio of 10:1 (EA/transfectant). The EAs were incubated with transfectants for 30 min at 37°C in culture media. Bound external EAs were either removed by hypotonic lysis in 0.25× PBS or labeled with a secondary fluorescent anti-IgG. In cells labeled with secondary fluorescent anti-IgG, external EAs become fluorescent, and internal EAs are not susceptible to the secondary labeling.

Lysosome Protein Labeling. Transfectants were allowed to internalize EAs for various times. After removal of the medium, 100% ice-cold methanol at −20°C was added for 20 min to fix and lyse the transfectants. Cells were washed with PBS then blocked with 3% BSA for 30 min. Anti-LAMP-1, Rab5, or Rab7 were added to the coverslips and incubated on ice for 30 min. The

This paper was submitted directly (Track II) to the PNAS office.

Abbreviations: CHO, Chinese hamster ovary; EA, antibody-coated cells; ER, endoplasmic reticulum; BAPTA-AM, 1,2-bis(2-aminophenoxy)ethane-*N*,*N*,*N*′,*N*′-tetraacetic acid tetra-(acetoxymethyl ester); LAMP-1, lysosome-associated protein 1.

§To whom correspondence should be addressed. E-mail: hpetty@umich.edu.

BIOPHYSICS

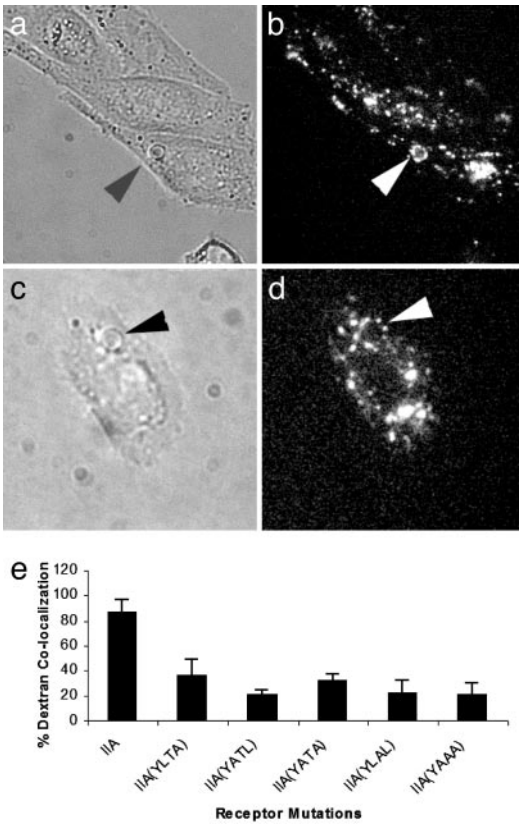

Fig. 1. Phagolysosome formation by CHO cells expressing WT or mutant forms of FcγRIIA. Cells were preloaded with rhodamine dextran. Cells were incubated with IgG-coated sheep erythrocytes (EA) for 30 min at 37°C then transferred to 4°C. External EA were labeled with fluorescent anti-IgG or removed by hypotonic lysis. Fluorescence microscopy was used to monitor the colocalization of rhodamine dextran with internalized targets. (*a* and *b*) Arrowheads indicate areas of colocalization of the internal EA with dextran in WT FcγRIIA cells. (*c* and *d*) Mutant FcγRIIA (AAA)-expressing cells; arrowheads point to internal EA that lack colocalization with dextran. (*e*) Quantitative data concerning the colocalization of EA with fluorescent dextran. In the WT FcγRIIA, ≈90% of targets were colocalized with dextran. However, mutation of the L-T-L motif reduced the percent of targets colocalized with dextran to levels previously obtained with a tailless form of FcγRIIA, suggesting that the L-T-L motif participates in phagolysosome fusion.

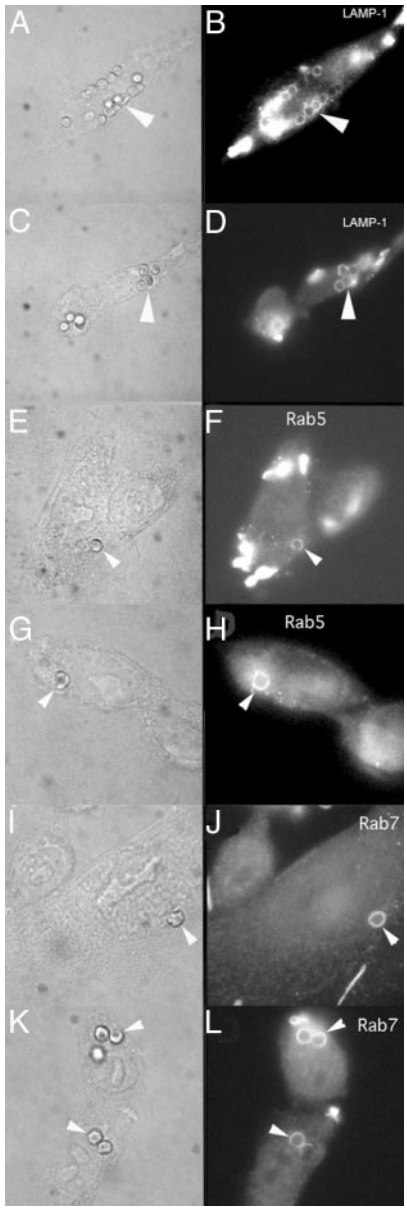

Fig. 2. Phagolysosome markers associated with FcγRIIA or mutant FcγRIIA (AAA). (*A–D*) Cells labeled with anti-LAMP-1, which is usually associated with late endosomal and phagosomal maturation. Shown are cells expressing WT FcγRIIA (*A* and *B*) or mutant FcγRIIA (AAA) (*C* and *D*). Colocalization of targets with LAMP-1. (*E–L*) Cells labeled with anti-Rab5 (*E–H*) and anti-Rab7 (*I–L*), which are early markers of phagolysosome maturation. Both markers colocalize with targets in cells expressing WT (*E*, *F*, *I*, and *J*) and mutant FcγRIIAs (*G*, *H*, *K*, and *L*).

transfectants were washed three times with PBS followed by labeling with tetramethylrhodamine isothiocyanate-conjugated antiisotype antibody for 30 min on ice, washed three times with PBS, and then observed by fluorescence microscopy.

Quantitative Microfluorometry. Transfectants were preloaded with Indo-1(AM) (Molecular Probes) for 60 min at 37°C. Cells were washed in PBS then mixed with EAs at 37°C. Fluorescence was detected by using an Axiovert 35 (Zeiss) coupled to a model D104 detection system (Photon Technology International, Lawrenceville, NJ) containing a Hamamatsu photomultiplier tube. Fluorescence intensities were recorded as a function of time by using FELIX software (Photon Technology International).

Spatiotemporal Analysis of Calcium Signals. Transfectants were loaded with Indo-1(AM) as described. They were mounted on coverslips then imaged with a cooled IMAX-intensified charge-coupled device camera (Princeton Instruments, Princeton) coupled to the bottom port of an Axiovert 135 microscope. A high-speed Princeton ST-133 interface and a Stanford Research (Sunnyvale, CA) delay gate generator controlled image acquisition (17–19). WINSPEC software (Princeton Instruments) was used.

Results

Identification of the L-T-L Phagolysosome Fusion Motif Within FcγRIIA. Using CHO cells transfected with FcγRIIA and CR3 in a reverse genetic complementation approach, it had been demonstrated that FcγRIIA's cytoplasmic domain contains information vital for phagolysosome formation (16). Therefore, we tested the hypothesis that an amino acid sequence within FcγRIIA's cytoplasmic domain participates in phagolysosome formation. Phagolysosome formation was detected by using the rhodamine-conjugated dextran procedure, which monitors fluid transfer

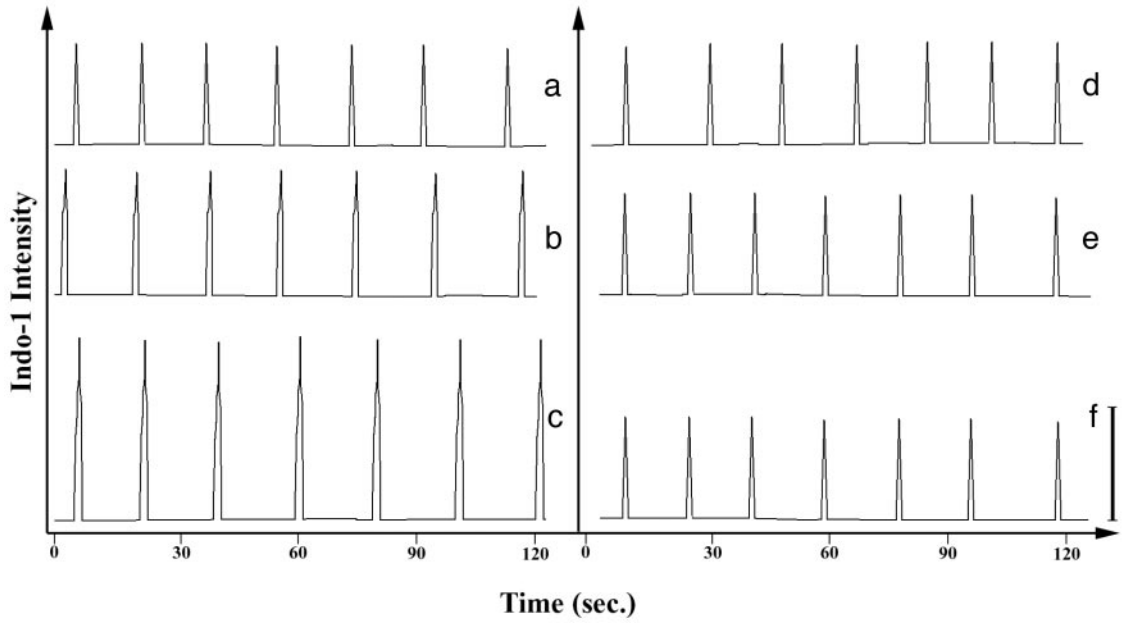

Fig. 3. Intracellular calcium concentration. Cells were preloaded with indo-1AM. Cells were placed on coverslips, then observed by using fluorescence microscopy. A photomultiplier tube attached to a Zeiss microscope was used to quantify the fluorescence intensity. Calcium spikes are observed in both WT and mutant FcγRIIA (*a* and *d*, respectively). Calcium spikes were also observed in cells after phagocytosis of one (*b* and *e*) or two (*c* and *f*) targets. Transfectants expressing WT FcγRIIA exhibited increases in calcium spike intensity after phagocytosis of IgG-opsonized targets (*b* and *c*). However, cells expressing FcγRIIA (AAA) did not display this increase in calcium amplitude (*e* and *f*). The bar at the lower right represents the calcium signal amplitude obtained in cells expressing WT FcγRIIA containing one internalized target.

between lysosomes and phagosomes (16). We discovered that mutation of the cytoplasmic L-T-L motif to A-A-A inhibited phagolysosome formation by >80% (Fig. 1). Mutation of either leucine residue inhibited phagolysosome fusion by >60% (Fig. 1). In addition, mutation of the threonine alone inhibited phagolysosome formation by >75%. In subsequent experiments we used the mutant FcγRIIA containing the L-T-L to A-A-A mutation, FcγRIIA (AAA), which reduces phagolysosome formation to levels comparable with a tailless mutant of FcγRIIA (Fig. 1; ref. 16).

Phagolysosome-Associated Proteins Are Recruited to Phagosomes in Cells Expressing WT and Mutant FcγRIIAs. We next sought to identify the mechanism responsible for the defective phagolysosome formation in cells expressing FcγRIIA (AAA). To accomplish this goal, we studied the acquisition of three phagolysosome maturation markers by phagosomes in CHO cells expressing WT FcγRIIA or FcγRIIA (AAA). We found that both WT FcγRIIA and FcγRIIA (AAA)-expressing transfectants (Fig. 2) acquired these markers of phagolysosome maturation. As illustrated in Fig. 2 *A–D*, a late marker of phagolysosome formation, LAMP-1, was recruited to phagosomes as well as the earlier markers Rab5 and Rab7 (Fig. 2 *E–L*). Hence, defective phagolysosome signaling associated with FcγRIIA (AAA) apparently lies downstream from these phagolysosome markers.

Chelation of Intracellular Calcium Inhibits FcγRIIA-Mediated Phagolysosome Fusion. Calcium is a key messenger in many cell functions, including phagosome-to-lysosome fusion (14, 15). Therefore, we examined the potential role of calcium in phagolysosome formation in these cells. Cells were incubated with the calcium chelator 1,2-bis(2-aminophenoxy)ethane-*N*,*N*,*N*′,*N*′-tetraacetic acid tetra(acetoxymethyl ester) (BAPTA-AM). BAPTA-AM enters cells, then becomes lipid-insoluble after cleavage of the acetoxymethyl ester group. Tetramethylrhodamine isothiocyanate-dextran-labeled cells were loaded with BAPTA, then allowed to internalize EA. In the presence of WT FcγRIIA, phagolysosome fusion was diminished by BAPTA in a dose-dependent manner. BAPTA at 5, 10, and 20 μM inhibited phagolysosome fusion by 30%, 40%, and 75%, respectively (data not shown). In addition, chelation of intracellular calcium by BAPTA did not affect the acquisition of lysosomal markers Rab5, Rab7, or LAMP-1 (data not shown), suggesting that calcium does not play a central role in the recruitment of these markers. These data suggest that calcium participates in phagolysosome fusion in this CHO cell transfectant system.

The L-T-L Motif Supports Enhanced Calcium Spike Amplitudes. Inasmuch as calcium participates in phagolysosome formation, we next examined the influence of the L-T-L to A-A-A mutation on calcium signaling in CHO transfectants with phagocytosed IgG-coated targets. Cells were labeled with indo-1, a calcium indicator that fluoresces when calcium is bound. Indo-1-labeled CHO cells expressing WT or mutant FcγRIIA display calcium spikes (Fig. 3 *a* and *d*). However, when one target is internalized by a transfectant, the amplitude of the calcium spike triggered by WT FcγRIIA is higher than that generated by FcγRIIA (AAA) (Fig. 3 *b* and *e*). In addition, on phagocytosis of multiple targets, the calcium spike amplitude in WT FcγRIIA-expressing cells increases according to the number of targets internalized. In contrast, FcγRIIA (AAA) cells do not show a change in calcium amplitude after phagocytosis. We suggest that this difference in calcium signaling is mechanistically linked to the deficiency in phagolysosome formation in FcγRIIA (AAA) cells.

The L-T-L Motif Affects Calcium Wave Propagation Patterns. To more clearly define the role of the L-T-L motif in calcium signaling, we performed high-speed microscopy experiments of indo-1-labeled transfectants. Spatial calcium waves have been observed during phagocytosis of IgG-coated targets by human neutrophils (19). We hypothesized that the signaling lesion of FcγRIIA (AAA) lies between the mechanistic steps of Rab7/LAMP-1

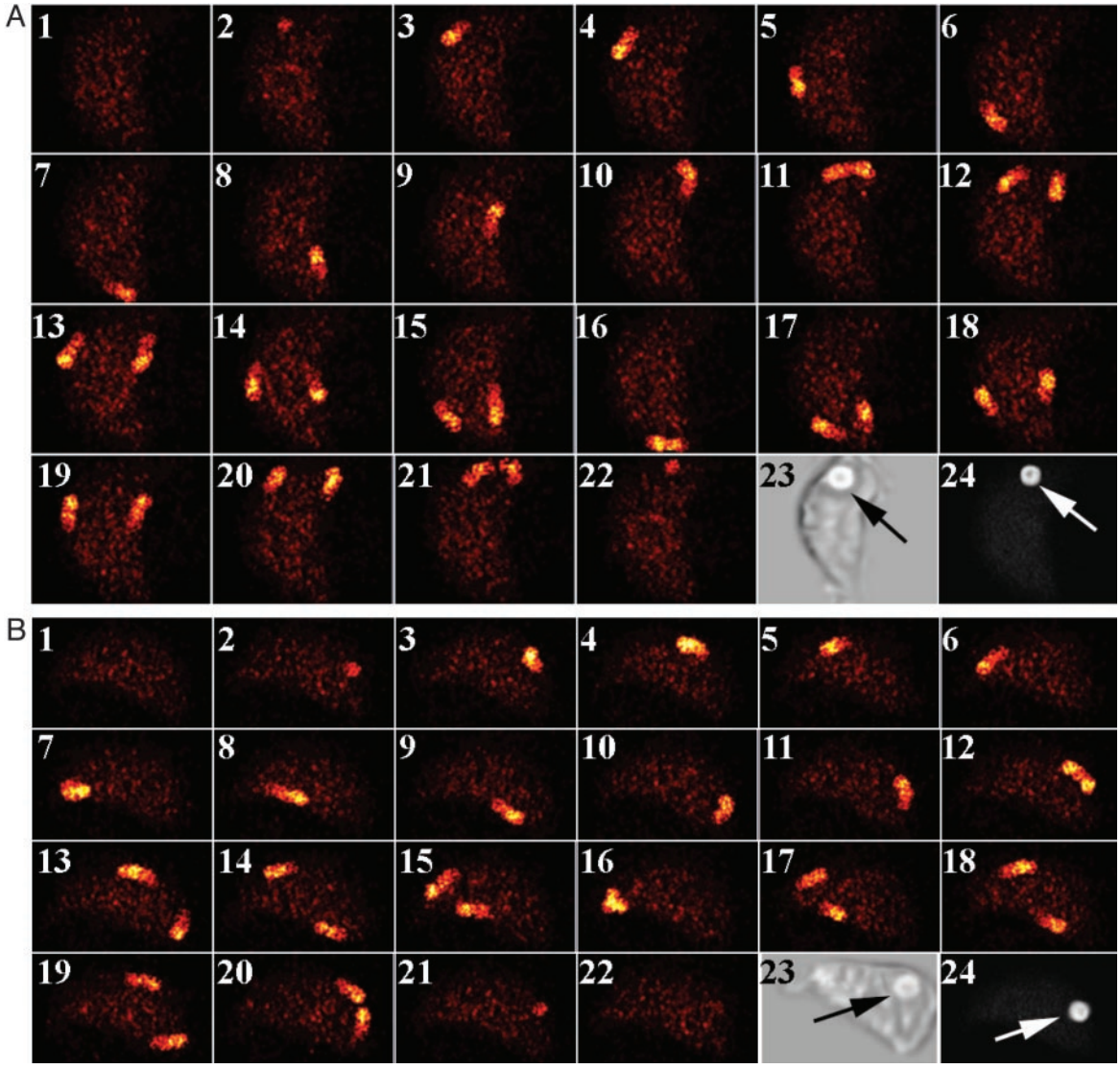

Fig. 4. The binding of IgG-opsonized targets triggers traveling calcium waves. High-speed fluorescence micrographs of indo-1-labeled cells were acquired by using a 100-nsec shutter speed and a 30-msec duty cycle (frames 1–22, *A* and *B*). Experiments were performed by using cells expressing WT FcγRIIA (*A*) and FcγRIIA (AAA) (*B*). For both the WT and mutant FcγRIIA, a calcium wave was initiated near the site of target binding. When this initial wave returns to the binding site, two calcium waves are observed propagating along the cell membrane that return to the site of target binding. Thus, no discernable differences exist in the calcium-signaling routes followed during IgG-opsonized target binding for these tranfectants. The locations of the IgG-opsonized erythrocytes (arrows) were confirmed by transmitted light microscopy in frame 23 of both *A* and *B*. After completion of the high-speed imaging, the extracellular locations of the targets were confirmed by labeling the opsonizing IgG on the target with a fluorescent anti-IgG second-step antibody. The FITC emission in frame 24 of both *A* and *B* demonstrates that the target was accessible to the second-step reagent. (Magnification: ×800.)

recruitment and calcium signaling. Using a previously described imaging system (17–19), we observed calcium wave propagation in transfectants expressing WT FcγRIIA or FcγRIIA (AAA). During the temporal interval of a calcium spike, a calcium wave(s) is observed in indo-1-labeled cells at brief exposure times (≈100 nsec) with a short delay between exposures (≈30 msec). When IgG-coated targets are bound to the surface of cells expressing either WT or AAA mutant FcγRIIA, the calcium wave patterns are indistinguishable (Fig. 4). In the absence of a bound target a single calcium wave is observed (data not shown), but in the presence of a target two calcium waves are observed propagating from the vicinity of the target (Fig. 4*A*, frame 11, and Fig. 4*B*, frame 12). The propagation of two calcium waves after receptor perturbation has also been observed for the fMet-Leu-Phe-mediated activation of neutrophils (19).

After WT FcγRIIA-mediated phagocytosis, a calcium wave travels around the plasma membrane toward the vicinity of the phagosome. When the wave nears the phagosome's vicinity, it separates into two distinct waves with one traveling once around the perimeter of the phagosome and the other continuing around the plasma membrane to the point of origin (Fig. 5*A*). This wave propagates every 20 sec and takes ≈200 msec to complete its journey around the cell. However, we observed a striking difference in the path of calcium travel in transfectants expressing FcγRIIA (AAA) (Fig. 5) after phagocytosis. As shown in Fig. 5*B*, when FcγRIIA (AAA) mediates phagocytosis, the calcium wave arises as in the WT FcγRIIA but fails to propagate normally about the phagosome when it reaches the vicinity of the target or "routing station" on the plasma membrane. Whereas the WT FcγRIIA switches the calcium wave to circle around the phagosome, the mutant FcγRIIA is unable to mediate this switching signal, and the calcium wave continues traveling past

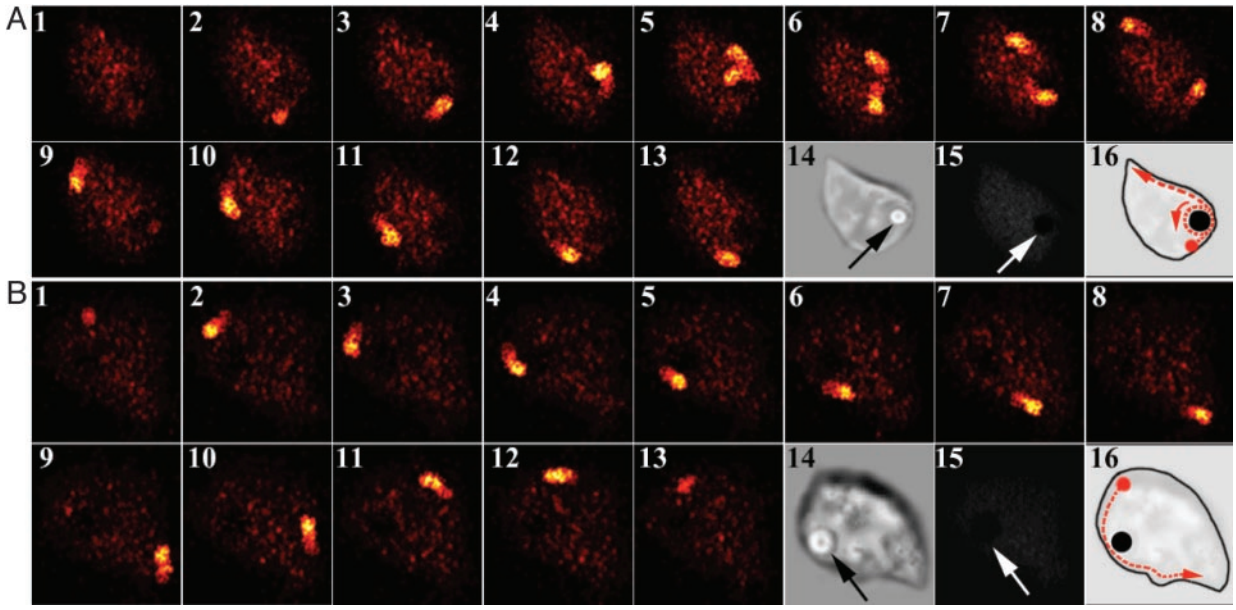

Fig. 5. Traveling calcium waves encircle phagosomes in transfectants expressing WT FcγRIIA but not FcγRIIA (AAA). Images were collected as described. Experiments were performed by using WT FcγRIIA (*A*) and FcγRIIA (AAA) (*B*). For transfectants expressing the WT FcγRIIA, the calcium wave was found to split near the phagosome with one wave traveling intracellularly whereas the original wave continued propagating about the cell periphery. However, FcγRIIA (AAA)-expressing cells did not display the second calcium wave propagating in the phagosome's vicinity. The locations of the IgG-opsonized erythrocytes were confirmed by transmitted light microscopy in frame 14 of both *A* and *B*. The targets' intracellular locations (arrows) were confirmed by labeling the opsonizing IgG on the target with a fluorescent anti-IgG second-step antibody. The lack of fluorescence emission in frame 15 of both *A* and *B* demonstrates that the target was not accessible to the second-step reagent. Schematic diagrams of the signaling routes are shown in frame 16 of both *A* and *B*. (Magnification: ×800.)

the phagosome on its path around the plasma membrane. The fact that multiple calcium wave patterns arise in the WT transfectants but not the FcγRIIA (AAA) mutants accounts for the quantitative changes in calcium signal amplitude in the microfluorometry experiments (Fig. 3). Moreover, the lack of a phagosome-associated calcium wave likely accounts for the defective phagolysosome formation in the FcγRIIA (AAA) mutants.

Discussion

Spatiotemporal pathways of chemical reactions and their control are emerging themes in chemical engineering and cellular and tissue biochemistry (17–22). In living cells these spatiotemporal chemical reactions often take the form of traveling chemical waves (17–19). Although purely physical systems can be controlled by size, physical perturbations such as temperature, and feedback, living cells are restricted largely to gene expression and feedback pathways. In the present study we have identified a specific sequence of three amino acids within the cytoplasmic region of FcγRIIA that controls the calcium wave pathway within living cells and, crucially, the ability of immune cells to destroy internalized targets via phagolysosome formation.

Previous studies have identified calcium waves in certain cell types including oocytes, myocytes, and retinal pigment epithelial cell monolayers (23–25). To observe waves in smaller cells, we have developed methods to collect movies of traveling chemical waves in cells by using brief shutter speeds (17–19). When IgG-opsonized targets bind to transfectants expressing FcγRIIA, two calcium waves emanate from the binding site, similar to that of other neutrophil-activating stimuli (19). When the two calcium waves collide on the far side of the cell (e.g., Fig. 3*A*), the waves do not annihilate. Although special conditions may permit traveling waves to "jump" the trailing refractory zones, it is more likely that the lack of annihilation is caused by different underlying biochemical mechanisms for each wave (19). After phagocytosis of a target, a calcium wave traveling about the perimeter of the cell and another calcium wave traveling about the perimeter of the phagosome are observed. We now show that organelle-to-organelle trafficking of calcium signals can depend on specific amino acid sequences within the receptor eliciting the biological response. Our studies have shown that the mutant receptor FcγRIIA (AAA), which retains the ability to mediate IgG-dependent phagocytosis, loses the ability to direct perimembrane calcium waves to the internal phagosome compartment. The calcium waves travel as a thin line, which we presume to be related to the endoplasmic reticulum (ER), from the plasma membrane to the phagosome. Recent studies have suggested that the ER participates in phagocytosis. Recruitment of ER to the site of phagocytosis has been suggested by studies showing the presence of ER-associated proteins on purified phagosomes (12) and the accumulation of GFP-labeled calreticulin and calnexin, two proteins of the ER, at the phagocytic cup (26). In addition, electron microscopy studies indicate that phagosomes maintain a thin filament of ER connecting them with the plasma membrane (27). This observation is significant in that the calcium signal from the plasma membrane to the phagosome often travels over a relatively long distance ($\approx$0.2–1 μm). We propose that the spindle of ER connecting the phagosome to the plasma membrane may be an "extension cord" linking the plasma membrane signaling apparatus to the phagosome, thus allowing calcium waves to travel to the phagosome. The mechanism linking perimembrane calcium waves to internal calcium waves may be analogous to that found in the sarcoplasmic reticulum of muscle. In this case plasma membrane L-type calcium channels are in direct contact with ryanodine receptors of the sarcoplasmic reticulum (28, 29). Furthermore, plasma membrane-to-phagosome communication remains intact for some time after phagocytosis, presumably to promote phagolysosome formation. The fact that ER is a storage site for intracellular calcium suggests that it would be an excellent source of calcium to regulate phagolysosome fusion. Other

studies have proposed a model whereby intracellular free calcium redistributes to the periphagosomal area in human neutrophils (30), which is consistent with the results reported above.

Our observations demonstrate two features of phagolysosome formation. First, we have identified a motif in the cytoplasmic domain of FcγRIIA required for normal phagolysosome fusion. Second, by using this mutant we have shown that this L-T-L motif is required for calcium signal routing to the phagosome, a key process leading to phagolysosome fusion. We anticipate that the powerful combination of molecular biological and high-speed imaging techniques will provide further insights into the nature of signal trafficking within living cells.

This work was supported by the National Institutes of Health (Grants CA74120 and AI 51789 to H.R.P., and Grants AI22193 and HL27068 to A.D.S.) and the National Multiple Sclerosis Society (to H.R.P.). R.G.W. is an Arthritis Foundation postdoctoral fellow.

1. Mayorga, L. S., Bertini, F. & Stahl, P. D. (1991) *J. Biol. Chem.* **266,** 6511–6517.
2. Mitchell, M. A., Huang, M.-M., Chien, P., Indik, Z. K., Pan, X. Q. & Schreiber, A. D. (1994) *Blood* **84,** 1753–1759.
3. Crowley, M. T., Costello, P. S., Fitzer-Attas, C. J., Turner, M., Meng, F., Lowell, C., Tybulewicz, V. L. & DeFranco, A. L. (1997) *J. Exp. Med.* **186,** 1027–1039.
4. Kiefer, F., Brumell, J., Al-Alawi, N., Latour, S., Cheng, A., Veillette, A., Grinstein, S. & Pawson, T. (1998) *Mol. Cell. Biol.* **18,** 4209–4220.
5. Tridandapani, S., Lyden, T. W., Smith, J. L., Carter, J. E., Coggeshall, K. M. & Anderson, C. L. (2000) *J. Biol. Chem.* **275,** 20480–20487.
6. Bonilla, F. A., Fujita, R. M., Pivniouk, V. I., Chan, A. C. & Geha, R. S. (2000) *Proc. Natl. Acad. Sci. USA* **97,** 1725–1730.
7. Kyono, W. T., de Jong, R., Park, R. K., Liu, Y., Heisterkamp, N., Groffen, J. & Durden, D. L. (1998) *J. Immunol.* **161,** 5555–5563.
8. Massol, P., Montcourrier, P., Guillemot, J. C. & Chavrier, P. (1998) *EMBO J.* **17,** 6219–6229.
9. Caron, E. & Hall, A. (1998) *Science* **282,** 1717–1721.
10. Hackam, D. J., Rotstein, O. D., Schreiber, A., Zhang, W. & Grinstein, S. (1997) *J. Exp. Med.* **186,** 955–966.
11. Desjardins, M., Huber, L. A., Parton, R. G. & Griffiths, G. (1994) *J. Cell Biol.* **124,** 677–688.
12. Garin, J., Diez, R., Kieffer, S., Dermine, J. F., Duclos, S., Gagnon, E., Sadoul, R., Rondeau, C. & Desjardins, M. (2001) *J. Cell Biol.* **152,** 165–180.
13. Downey, G. P., Botelho, R. J., Butler, J. R., Moltyaner, Y., Chien, P., Schreiber, A. D. & Grinstein, S. (1999) *J. Biol. Chem.* **274,** 28436–28444.
14. Carafoli, E. (2002) *Proc. Natl. Acad. Sci. USA* **99,** 1115–1122.
15. Malik, Z. A., Denning, G. M. & Kusner, D. J. (2000) *J. Exp. Med.* **191,** 287–302.
16. Worth, R. G., Mayo-Bond, L., Kim, M. K., van de Winkel, J. G., Todd, R. F., Petty, H. R. & Schreiber, A. D. (2001) *Blood* **98,** 3429–3434.
17. Kindzelskii, A. L. & Petty, H. R. (2002) *Proc. Natl. Acad. Sci. USA* **99,** 9207–9212.
18. Petty, H. R., Worth, R. G. & Kindzelskii, A. L. (2000) *Phys. Rev. Lett.* **84,** 2754–2757.
19. Kindzelskii, A. L. & Petty, H. R. (2003) *J. Immunol.* **170,** 64–72.
20. Wolff, J., Papathanasiou, G., Kevrekidis, I. G., Rotermund, H. H. & Ertl, G. (2001) *Science* **294,** 134–137.
21. Sakurai, T., Mihaliuk, E., Chirila, F. & Showalter, K. (2002) *Science* **296,** 2009–2012.
22. Gluckman, B. J., Nguyen, Weinstein, S. L. & Schiff, S. J. (2001) *J. Neurosci.* **21,** 590–600.
23. Lechleiter, J. D. & Clapham, D. E. (1992) *Cell* **69,** 283–294.
24. Wussling, M. H. P. & Salz, H. (1996) *Biophys. J.* **70,** 1144–1153.
25. Newman, E. & Zahs, K. R. (1997) *Science* **275,** 844–847.
26. Muller-Taubenberger, A., Lupas, A. N., Li, H., Ecke, M., Simmeth, E. & Gerisch, G. (2001) *EMBO J.* **20,** 6772–6782.
27. Gagnon, E., Duclos, S., Rondeau, C., Chevet, E., Cameron, P. H., Steele-Mortimer, O., Paiement, J., Bergeron, J. J. & Desjardins, M. (2002) *Cell* **110,** 119–131.
28. Stendahl, O., Krause, K. H., Krischer, J., Jerstrom, P., Theler, J. M., Clark, R. A., Carpentier, J. L. & Lew, D. P. (1994) *Science* **265,** 1439–1441.
29. Lew, D. P., Andersson, T., Hed, J., Di Virgilio, F., Pozzan, T. & Stendahl, O. (1985) *Nature* **315,** 509–511.
30. Jaconi, M. E., Lew, D. P., Carpentier, J. L., Magnusson, K. E., Sjogren, M. & Stendahl, O. (1990) *J. Cell Biol.* **110,** 1555–1564.